Influence of preparation methods and nanomaterials on hydrophobicity and anti-icing performance of nanoparticle/epoxy coatings

Shinan Liu , Houzhi Wang * , Yixuan Liu , Yunhong Yu , Yuxiang Li , Jun Yang , Lefei Huang

Posted Date: 15 September 2023

doi: 10.20944/preprints202309.0981.v1

Keywords: Hydrophobic coating; Nanoparticles; Ice Adhesion Force; Contact Angle; Asphalt concrete

Article

Influence of Preparation Methods and Nanomaterials on Hydrophobicity and Anti-Icing Performance of Nanoparticle/Epoxy Coatings

Shinan Liu [a], Houzhi Wang [a,*], Yixuan Liu [a], Yunhong Yu [a], Yuxiang Li [a], Jun Yang [a] and Lefei Huang [a]

[a] School of Transportation, Southeast University, Nanjing 211189, China
* Correspondence: houzhi_wang@seu.edu.cn

Abstract: Despite their anti-icing ability, hydrophobic coatings have the disadvantages of easy falling off and poor wear resistance, resulting in insufficient durability of ice/snow melting. To improve the surface stability and durability of superhydrophobic coatings, nanoparticle/epoxy coatings were prepared with three types of nanoparticles, two types of dispersion methods, three types of application methods and two types of introduction methods of epoxy resin. Water contact angles, ice adhesion force and icing rate of asphalt concrete coated with hydrophobic coatings were tested. The molecular structures of coatings were analyzed by Fourier transform infrared spectroscopy. The surface morphology of hydrophobic coatings was observed using Scanning electron microscopy. Results indicated that nano-ZnO, TiO_2 and SiO_2 particles can be modified into hydrophobicity by stearic acid. The hydrophobic coating could improve the hydrophobicity of concrete, reduce the adhesion strength of ice and asphalt concrete and delay the beginning icing time. Moreover, The dosages of stearic acid, nanoparticle and epoxy resin need to be in a certain range to ensure the best hydrophobicity and durability of coatings.

Keywords: hydrophobic coating; nanoparticles; ice adhesion force; contact angle; asphalt concrete

1. Introduction

In winter, most expressways face the problem of road icing, which significantly reduces the friction coefficient of the road surface and leads to serious traffic accidents. In addition, the resulting freeze–thaw damage may shorten the road lifespan. Moreover, because the surface of the concrete is porous, water enters the surface. In particular, the water in the pores freezes and expands, resulting in tensile stress inside the concrete and cracking of the concrete. Furthermore, the ice in the pores is integrated with the surface ice; consequently, the ice is firmly attached to the concrete surface, which hampers deicing.

For the problem that concrete pavement is easy to freeze and difficult to remove ice, a great deal of research has been conducted on the icing behavior of concrete road surfaces, and many active anti-icing and passive deicing technologies for concrete pavement have been applied[1–3]. The active anti-icing method consists in modifying the traditional material and structural design of the pavement before icing occurs. This approach mainly yields self-stress elastic pavement, low-freezing-point pavement, and energy conversion pavement. However, these technologies are not widely used owing to their capital cost and construction difficulty. The passive deicing method consists in removing the ice by physical and chemical means when icing is complete. This approach is mainly categorized into the mechanical deicing and the chemical agent deicing. Research and engineering practice have proved that passive deicing not only damages the road surface seriously but also has short-term effect.

Removing water from the concrete prevents the freezing of the concrete surface totally. Superhydrophobic coatings [4–8] are waterproof, antifog, and anti-icing and are widely used in

aerospace, power communication, etc. However, few hydrophobic coating technologies are applied to road surfaces. In 1997, German botanist Barthlott [9] found that the surface of lotus leaves has strong hydrophobicity and self-cleaning ability; this captured the attention of scholars worldwide, who carried out in-depth research on hydrophobic materials. In 2002, Laforte [10] first discovered that superhydrophobic coatings can reduce the ice adhesion to the substrate, and the hydrophobic anti-icing technology has developed rapidly since then. Arabzadeh et al. [11] mixed polytetrafluoroethylene, epoxy resin, and acetone to obtain a superhydrophobic coating for pavement, which has a good anti-icing effect. Ruan [12] prepared an anti-icing hydrophobic coating on the surface of an aluminum alloy substrate. The produced hydrophobic surface did not start to freeze until the temperature reached −8 °C, indicating that it can reduce the freezing temperature. Yang [13] prepared a hydrophobic coating on an aluminum surface and achieved significant anti-icing properties; in particular, the surface icing was greatly delayed. Antonini [14] used an aluminum substrate to study the effect of hydrophobic coatings on the anti-icing of aircraft wings. The results showed that a hydrophobic coating can reduce not only the wing icing but also the energy used to deice the wing (by 80%). Dotan [15] studied the relationship between water wettability and ice adhesion. Various polycarbonate-coated surfaces were obtained through appropriate chemical methods, including superhydrophilic and superhydrophobic surfaces. Ice adhesion tests and contact angle measurements showed that the larger the contact angle, the lower the ice adhesion. The best results were obtained in the case of superhydrophobic surface treatments, where ice adhesion was significantly reduced compared to untreated aluminum surfaces. However, the main focus of current research on superhydrophobic nanocoatings is metal anticorrosive rather than road anti-icing coatings [16,17]. On account of the different characteristics of asphalt concrete, cement concrete, and metal substrates, road anti-icing coatings require further research.

The addition of polar nanoparticles can reduce the surface energy and enhance the hydrophobicity of the coating [18]. However, the high surface energy of nanoparticles prevents them from dispersing uniformly in organic media, which limits the application of nanocoatings [19,20]. To solve this problem, researchers found that the organic modification of nanoparticle surface can achieve a better dispersion effect [21–24].

Existing studies show that improving the hydrophobicity of the coating and the adhesion between the coating and the road surface can achieve good deicing performance and durability. However, the current research on the application of hydrophobic materials for road anti-ice condensation is mostly limited to laboratory experiments, and few coating technologies are used in physical engineering and are recognized and promoted. This is because the superhydrophobic coating material is brittle and susceptible to wear, has weak adhesion to the road surface, is easy to fall off, and has poor surface stability, which leads to insufficient durability of the ice and snow melting function [25,26]. Therefore, to solve the defects of coating technology, epoxy and nanomaterial coatings were designed and prepared in this study not only to realize the anti-icing and deicing of pavement but also to improve the wear, water, and impact resistance of pavement coating. Further, there are few evaluation methods for the anti-icing performance of coatings and few repeatable and standardized test methods that can quantitatively analyze the anti-icing performance of coatings or pavements. Through evaluation tests of anti-icing performance, a quantitative and reproducible evaluation method for the anti-icing performance of coatings and a test platform were developed in this study. Based on the proposed method, the anti-icing performance of the hydrophobic epoxy coating was tested at low temperatures and the anti-icing performance mechanism of coatings was explored from the perspective of microstructure.

In this study, nanoparticle/epoxy coatings were prepared with three types of nanoparticles, two types of dispersion methods, three types of application methods and two types of introduction methods of epoxy resin. Water contact angles, ice adhesion force and icing rate of asphalt concrete coated with hydrophobic coatings were tested. The molecular structures of coatings were analyzed by Fourier transform infrared spectroscopy. The surface morphology of hydrophobic coatings was observed using Scanning electron microscopy. Finally, the anti-icing mechanism of the coating was discussed.

 doi:10.20944/preprints202309.0981.v1

2. Materials and methods

2.1. Raw materials

ZnO, TiO_2, and SiO_2 nanoparticles were used as the main component for hydrophobic coatings. Epoxy resin was employed for two functions: (1) To improve the wear, water, and impact resistance of the coating, epoxy resin was mixed with hydrophobic materials as paint and diluent; (2) To improve the bonding between the coating and pavement, epoxy resin adhesive layer was employed between the hydrophobic coating slurry and the pavement surface. Stearic acid was used as a modifier for ZnO, TiO_2, and SiO_2 nanoparticles. The AC-16 grading was applied for the asphalt mixture in the preparation of Marshall specimen. The diameter of the specimen is 101.6 mm and the height of the specimen is 63.5 mm.

2.2. Preparation of the nanoparticle hydrophobic materials

The detailed preparation steps of the nanoparticle hydrophobic materials are as follows:

Different amounts of stearic acid granules were dissolved in 100 ml absolute ethanol to form a transparent stearic acid absolute ethanol solution. Afterward, 5g hydrophobic nanoparticles were added to the stearic acid absolute ethanol solution, which was stirred in a magnetic stirrer (MS) for 3 h until the nanoparticles were completely dissolved to form a milky white solution. Similarly, another solution was stirred by ultrasonic dispersion (UD) instrument, and the solution was completely dissolved after 10 min.

2.3. Preparation of the hydrophobic coatings

2.3.1. Application method

In this study, to determine the optimum preparation method for the hydrophobic coatings, the spraying, dipping, and brushing methods were used to apply the hydrophobic materials.

Spraying method (SM): Dust and other pollutants were removed from the surface of the glass slide, which was dried thereupon. Spraying was carried out with a spray gun. The zinc oxide stearic acid solution was poured into the spray gun. The pressure of the spray gun was set to 3 MPa. The vertical distance of spraying was 50 cm away from the glass slide, and the spray gun was kept downward and vertical. The glass slide was sprayed continuously for 15 s (10 times) and thereafter kept at 25°C for 24 h.

Dipping method (DM): Dust and other pollutants were removed from the surface of the glass slide, which was dried thereupon. The clean glass slide was immersed in the zinc oxide stearic acid solution for 30 s and thereafter kept at 25°C for 24 h.

Brushing method (BM): Dust and other pollutants were removed from the surface of the glass slide, which was dried thereupon. A certain amount of zinc oxide stearic acid solution was brushed on the glass slide three times to ensure that the coating was evenly distributed on the surface of the glass slide. Afterward, the glass slide was kept at 25°C for 24 h.

2.3.2. Preparation of coated Marshall specimens

Epoxy resin has excellent physical and mechanical properties, electrical insulation properties, and adhesion properties with various materials. Therefore, it is used in coatings, composites, castings, adhesives, molding materials, and injection molding materials. Epoxy resin confers good strength and durability on the coating, but it is easy to crack and has poor impact resistance owing to its high stiffness, especially in a low-temperature environment.

Therefore, a nanoparticle/epoxy composite coating was prepared in this study. The epoxy resin improved the coating durability, and the hydrophobic nanomaterials ensured the hydrophobicity and anti-icing properties of the coating, so that the coating could meet the road performance.

For the two functions of epoxy resin, two preparation methods of coated Marshall specimens were designed.

Preprints (www.preprints.org) | NOT PEER-REVIEWED | Posted: 15 September 2023 doi:10.20944/preprints202309.0981.v1

(1) Preparation of nanoparticle/epoxy hybrid coatings

First, 5g epoxy resin was introduced into the hydrophobic materials and the mixed solution was dispersed by magnetic stirrer for 10 min. Then, coating slurry was applied on the surface of Marshall specimen by the optimum preparation method. The mass of each substance in the hydrophobic materials was shown in Table 1.

Table 1. The mass of each substance in the hydrophobic materials.

Sample		nanoparticle(g)	Stearic acid (g)	Anhydrous ethanol (ml)	Epoxy resin(g)
ZnO-1		5	0.30	100	5
ZnO-2		5	0.40	100	5
ZnO-3	ZnO(g)	5	0.50	100	5
ZnO-4		5	0.60	100	5
ZnO-5		5	0.70	100	5
SiO_2-1		5	0.6	100	5
SiO_2-2		5	0.7	100	5
SiO_2-3	SiO_2(g)	5	0.8	100	5
SiO_2-4		5	0.9	100	5
SiO_2-5		5	1.00	100	5
TiO_2-1		5	0.25	100	5
TiO_2-2		5	0.50	100	5
TiO_2-3	TiO_2(g)	5	0.75	100	5
TiO_2-4		5	1.00	100	5
TiO_2-5		5	1.25	100	5

(2) Preparation of ZnO/epoxy layered coating

First, apply 5g epoxy resin on the surface of Marshall specimen, and then apply a certain amount of hydrophobic material after the epoxy resin began to cure and had a certain viscosity.

2.4. Characterization of superhydrophobic materials and coatings

In this study, the coating hydrophobicity was characterized by the contact angle. The volume of the liquid used for each measurement was 4 μl, and three different positions were taken for the contact angle test.

The microstructures of the superhydrophobic materials were observed by field-emission scanning electron microscopy (FESEM, Nova Nano SEM 450) with an accuracy of up to 30 nm. Because the measurements required objects with high conductivity, a metal layer was placed on the superhydrophobic coating before the observation.

The chemical structures of samples were characterized by FTIR spectroscopy (Nicolet iS10).

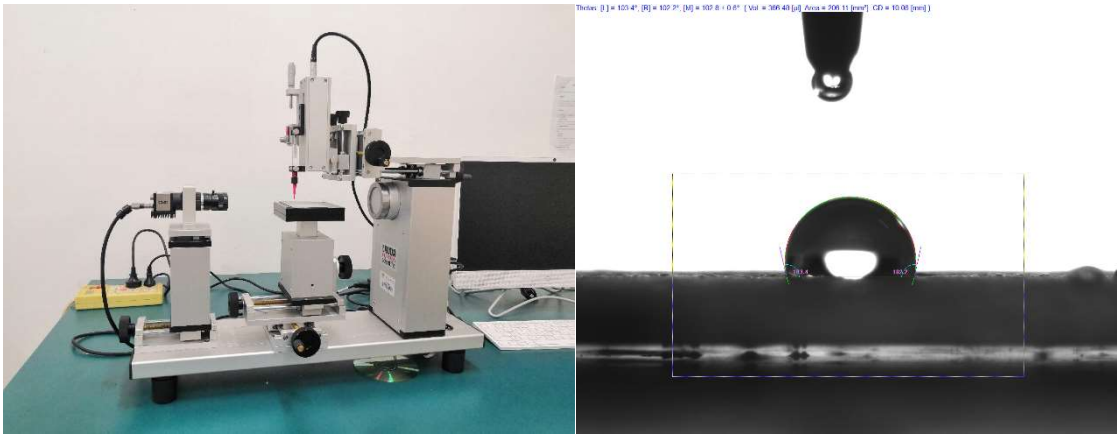

Figure 1. Left) Contact angle detector. (Right) Contact angle.

 doi:10.20944/preprints202309.0981.v1

2.5. Adhesion test

The efficacy of coatings has been evaluated by the adhesion force of the ice layer to the road surface and ice area to characterize the pavement force to remove ice layer with the iced pavement. A reproducible and quantitative method was designed to test the ice adhesion force on the surface and realize the quantitative evaluation of the anti-icing performance of the pavement. To meet the requirements of the simulation of real-road deicing and quantitative data, a set of test equipment was designed to simulate manual deicing. The anti-icing performance of the road surface was characterized by the maximum force during shoveling the accreted ice in a specific area.

The design includes the following three points:

(1) Simulation of manual deicing

In the anti-icing evaluation test, the damage of the ice-covered layer consists in vertical pullout damage and horizontal shear damage. These two types, especially the vertical pullout damage, are quite different from those of manual deicing. The vertical pullout damage is caused by applying a vertical pulling force between the ice layer and the road surface. Since there is no horizontal component force, the force required to destroy the bond between the ice layer and the road surface is much larger than that required for deicing. A road can be deiced by exerting a lateral force on the ice-covered layer to the road surface at a certain angle (30°), and the resultant damage is the combined effect of vertical pulling force and horizontal shear force. Therefore, to be practical, this study customized a 50 × 50-mm blade, which was placed at an angle of 30° to the horizontal and was connected to a 750 mm cylindrical steel pipe; the pipe was connected to the controller to move horizontally. The simulation of manual deicing was controlled by the blade. In particular, when the blade removed the ice, the manual deicing was simulated.

(2) Measurement of surface ice adhesion

The other end of the steel pipe was connected to a dynamometer, which was placed on the mobile device of the controller, and deicing was dynamically measured in real time through the computer software handheld recording tool.

(3) Formation of ice-covered layer and control of the quantitative area

To simulate the freezing and low-temperature environment in winter, the test specimens (Marshall specimens) were first pre-frozen in a low-temperature environment for 15 h, simulating the winter road surface. To control the ice-covered layer to reach a quantitative area, the Marshall specimen was wrapped with tin foil to create a cylindrical water tank and seal it to prevent water from flowing out. Subsequently, the water was dripped on the surface of the test specimen until the thickness of the ice layer reached 2 cm. The specimens were frozen for 5 h at -10℃ until the ice layer was completely condensed on the surface.

Preprints (www.preprints.org) | NOT PEER-REVIEWED | Posted: 15 September 2023 doi:10.20944/preprints202309.0981.v1

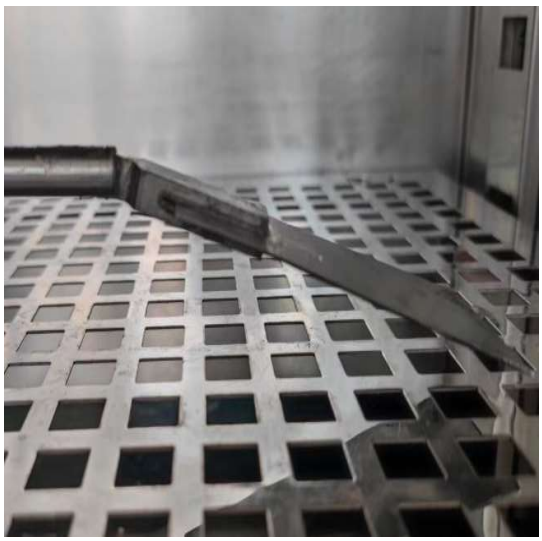

(a)

(b)

(c)

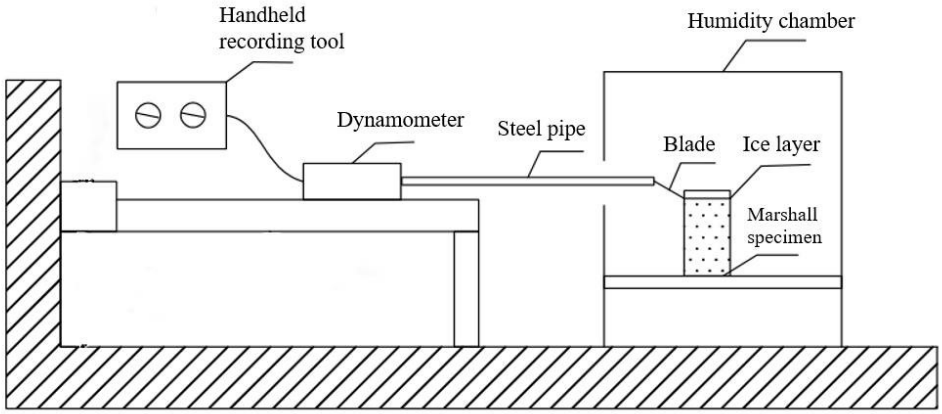

(d)

Figure 2. Evaluation method for adhesion force: (a)blade; (b) iced Marshall specimen; and (c) (d) experiment instrument.

 doi:10.20944/preprints202309.0981.v1

2.6. Simulation test of icing

As evaluation indexes of anti-icing performance, the amount and speed of road icing significantly influence the low-temperature safety and performance of the pavement. In this experiment, the anti-icing performance of hydrophobic coating on asphalt concrete was studied by simulating the icing of pavement surface gathered water.

The beginning icing time of water was observed on the different hydrophobic surfaces of asphalt concrete to investigate the icing delay function of hydrophobic coatings. Several groups of coated and uncoated specimens were prepared and put into the constant temperature and humidity box at −10, −6, and −2 ℃ for 5h. Then 15 g of water was dripped on the surface of the Marshall specimen wrapped with tin foil. Subsequently, the beginning icing time of these specimens was observed using a digital camera, and export and weigh the unfrozen water every 30min to calculate the icing rate.

2.7. Durability test of coatings

Epoxy resin provides primary durability in coating. To study the effect of epoxy resin content on the durability of different coatings, the durability test was carried out on an experimental road with a traffic flow of 3000pcu/d. The mass ratio of nanoparticles to stearic acid and the dosage of nanoparticle to hydrophobic materials were set to the optimum value. Coatings with different epoxy contents in sizes of 50 cm × 50 cm were applied on the asphalt pavement. Take samples from these coatings every 15 days and test their contact angles.

3. Results and discussion

3.1. Determination of the optimum preparation method

3.1.1. Dispersion method

To determine the optimum dispersion method, the contact angles of the ZnO nanoparticle hydrophobic materials coatings dispersed by the magnetic stirrer (MS) and ultrasonic dispersion (UD) instrument were measured. The spraying method was used for application.

As shown in Figure 3, The contact angles of the coatings prepared by ultrasonic dispersion were less than magnetic stirring, which shows that both preparation methods had a great influence on the hydrophobicity of the coating. The optimum mass ratios of nanoparticles to stearic acid of hydrophobic materials dispersed by MS and UD were the same, indicating that the dispersion method did not influence the optimum mass ratios of nanoparticles to stearic acid of hydrophobic materials.

Preprints (www.preprints.org) | NOT PEER-REVIEWED | Posted: 15 September 2023 doi:10.20944/preprints202309.0981.v1

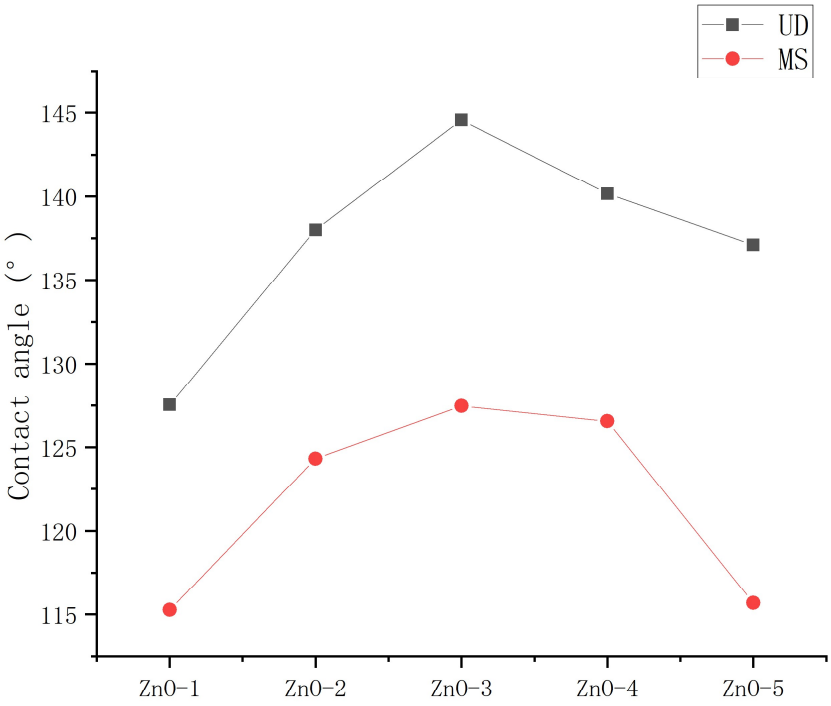

Figure 3. Contact angles of ZnO hydrophobic materials dispersed by MS and UD.

As shown in Figure 4, the ultrasonically dispersed solution was homogeneous but the magnetically stirred solution had obvious stratification. There are three possible reasons: 1. The ultrasonic disperser can reduce the particle size. When the particles are small enough, they are suspended in the liquid owing to buoyancy, making the solution homogeneous, whereas the particle size of the material prepared by magnetic stirring is larger, and precipitation occurs over time. 2. In contrast to magnetic stirring, the solution prepared by ultrasonic dispersion produces new chemical material. 3. The combined effect of the first and second reasons.

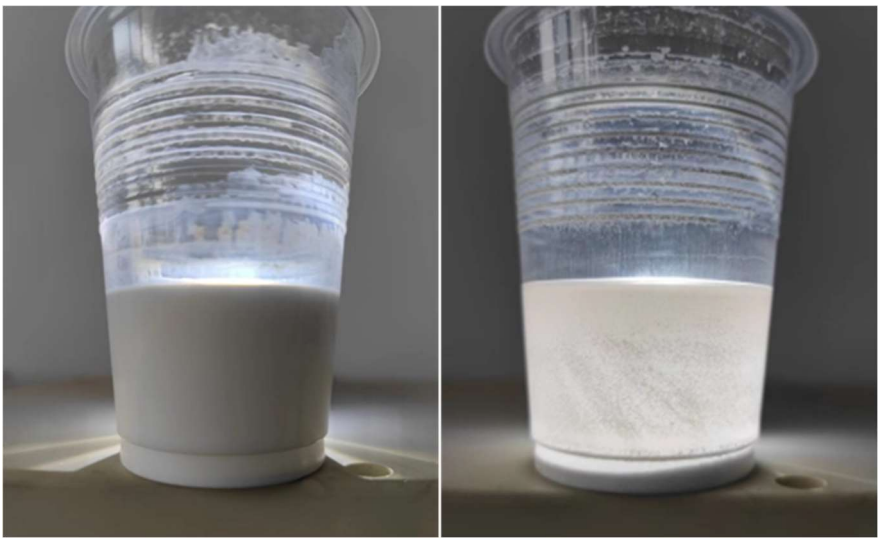

Figure 4. Ultrasonically dispersed (left) and magnetically stirred (right) ZnO-3 sample (after standing for 24 h).

Preprints (www.preprints.org) | NOT PEER-REVIEWED | Posted: 15 September 2023 doi:10.20944/preprints202309.0981.v1

To further explore the differences between the two solution dispersion methods, FTIR analysis of zinc oxide nanoparticles, magnetically stirred zinc oxide stearic acid particles, and ultrasonically dispersed zinc oxide stearic acid particles was carried out.

As shown in Figure 5, the peaks at 2919 and 2850 cm^{-1} were assigned to the asymmetric stretching vibration absorption of C–H of the alkyl group in stearic acid, indicating that the alkyl group in stearic acid was grafted onto the surface of ZnO particles [27]. In addition, the area of C–H peak of the ultrasonically dispersed, magnetically stirred, and not processed solutions showed a decreasing trend, indicating that the reaction degree of the three kinds of samples gradually decreased. The peak at 1707 cm^{-1} was assigned to the stretching vibration absorption of C=O. Since the absorption peak of the C=O functional group is a typical absorption peak in the molecular structure of stearic acid [28], the existence of C=O functional group in the FTIR spectra of modified zinc oxide indicates that stearic acid was successfully attached to the ZnO surface. The peaks at 1536 and 1462 cm^{-1} were assigned to the asymmetric and symmetric, respectively, stretching vibration of COO^- functional group, indicating the presence of the product of the stearic acid reaction on the surface of zinc oxide [29,30]. In contrast, these characteristic peaks did not appear in the FTIR spectra of the magnetically stirred and not processed solutions, indicating that stearic acid did not react significantly with ZnO.

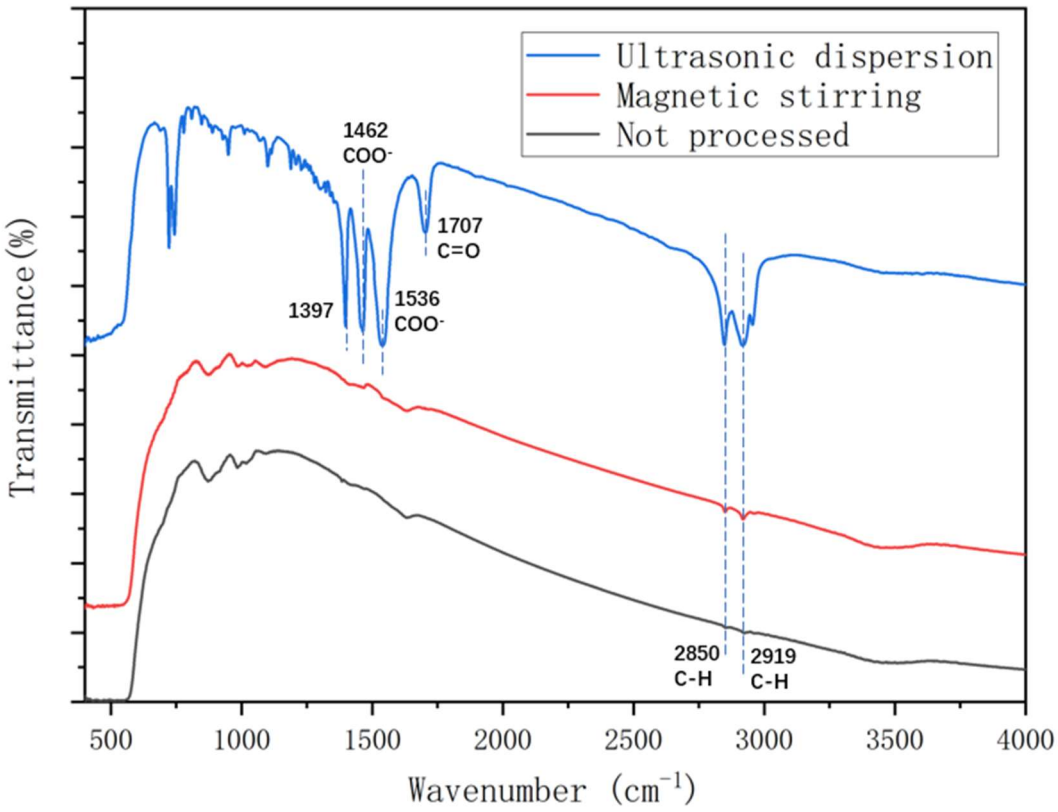

Figure 5. Fourier-transform infrared (FTIR) spectra for zinc oxide particles and modified zinc oxide particles by different preparation methods of coating solution.

The analysis of FTIR spectra confirmed that chemical reactions occurred when ZnO was mixed with stearic acid, which caused ZnO nanoparticles to disperse in the solvent more efficiently and reduced the surface energy of the coating. In addition, the reaction degree of not processed, magnetically stirred, and ultrasonically dispersed samples increased successively. The main reaction between zinc oxide and stearic acid can be expressed as follows [28]:

$$HO - ZnO - OH + CH_3(CH_2)_{16}COOH \rightarrow CH_3(CH_2)_{16}COO - ZnO - OOC(CH_2)_{16}\ CH_3 + H_2O$$

Preprints (www.preprints.org) | NOT PEER-REVIEWED | Posted: 15 September 2023 doi:10.20944/preprints202309.0981.v1

Compared to magnetic stirring, ultrasonic dispersion could greatly shorten the preparation time and improve the coating performance. Therefore, ultrasonic dispersion was selected as the optimal dispersion method of the coating solution.

3.1.2. Application method

To determine the optimum application method, the contact angles of the ZnO nanoparticle hydrophobic materials coatings applied by spraying, dipping, and brushing methods were measured. The ultrasonic dispersion (UD) instrument method was used for dispersion.

As shown in Figure 6, The hydrophobicity of coatings prepared by spraying, dipping and brushing methods decreased successively. Moreover, the optimum mass ratios of nanoparticles to stearic acid of hydrophobic materials applied by spraying, dipping, and brushing methods were the same, indicating that application method did not influence the optimum mass ratios of nanoparticles to stearic acid of hydrophobic materials.

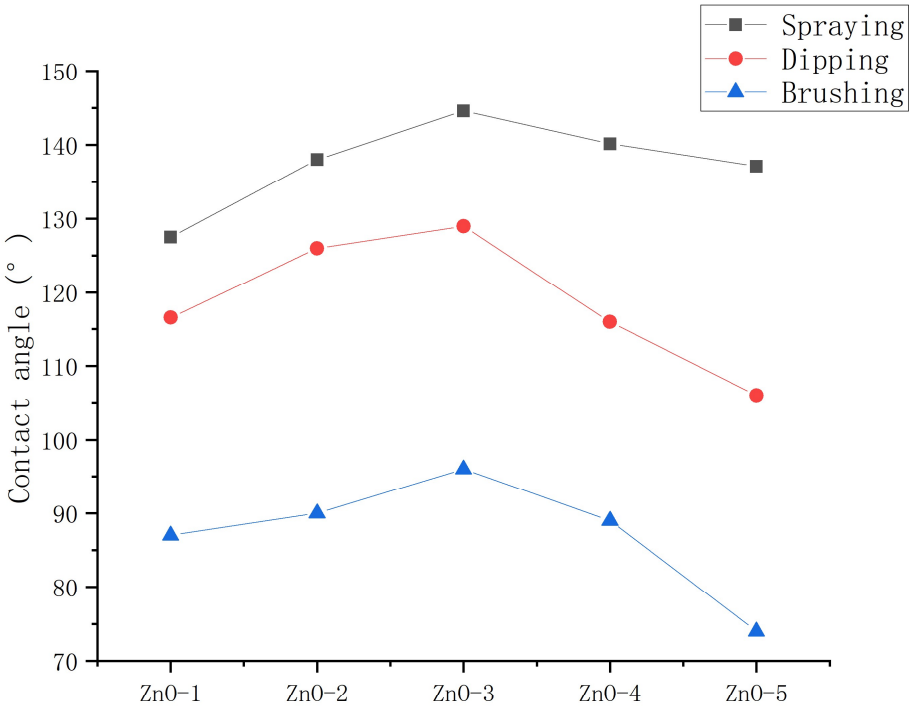

Figure 6. Contact angles of ZnO hydrophobic materials applied by spraying, dipping and brushing methods.

As shown in Figure 7, the coating prepared by the spraying method was even, it had a consistent thickness, and its surface was a milky white film. Moreover, the contact angle data at each position had small discreteness, indicating that its hydrophobicity was uniform. The coating prepared by the dipping method was uneven; the nanomaterials in the middle part were more. Further, some materials agglomerated to form milky white bumps, which was not conducive to the hydrophobicity of the coating. In addition, some areas were not available for contact angle measurement, and the contact angle data at each position had large discreteness. The surface of the coating prepared by the brushing method was uneven and had many milky white protrusions; in particular, the material aggregated more at the edges. Moreover, the overall coating was thick, and most areas were unavailable for contact angle measurement.

 doi:10.20944/preprints202309.0981.v1

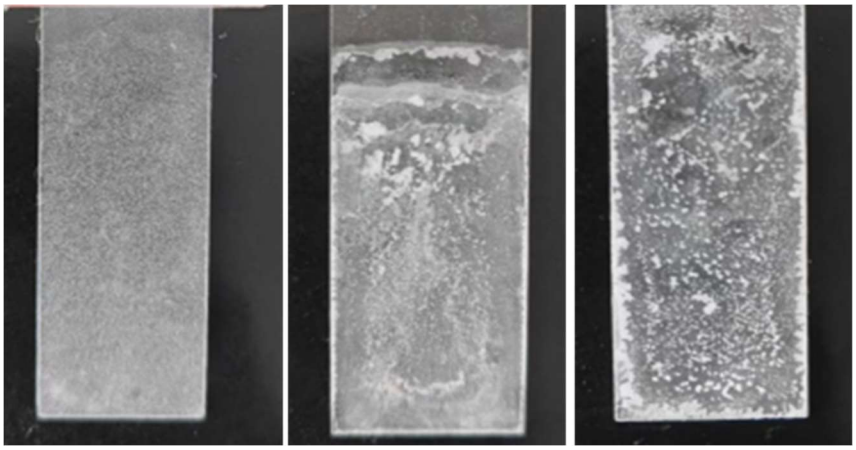

Figure 7. Surface morphology of spraying (left), dipping (middle), and brushing (right) methods.

From the perspective of engineering practice, only the spraying and brushing methods were applicable. Moreover, the spraying method had better hydrophobicity and was more economical than the brushing method. Therefore, the spraying method was designated as the optimal method to apply the solution.

To sum up, the best method for coating preparation consisted of ultrasonic dispersion and spraying.

3.1.3. Introduction method of epoxy resin

To determine the optimum introduction method of epoxy resin, the contact angles of the ZnO/epoxy hybrid coating and ZnO/epoxy layered coating were measured. The ultrasonic dispersion (UD) instrument method was used for dispersion. The spraying method was used for application.

As shown in Figure 8, the hydrophobicity and durability of the layered coatings were significantly better than those of hybrid coatings. Possibly, on account of the layered arrangement, the epoxy resin did not coat the nanoparticles and the nanoparticles could be exposed to shape the rough surface.

Preprints (www.preprints.org) | NOT PEER-REVIEWED | Posted: 15 September 2023 doi:10.20944/preprints202309.0981.v1

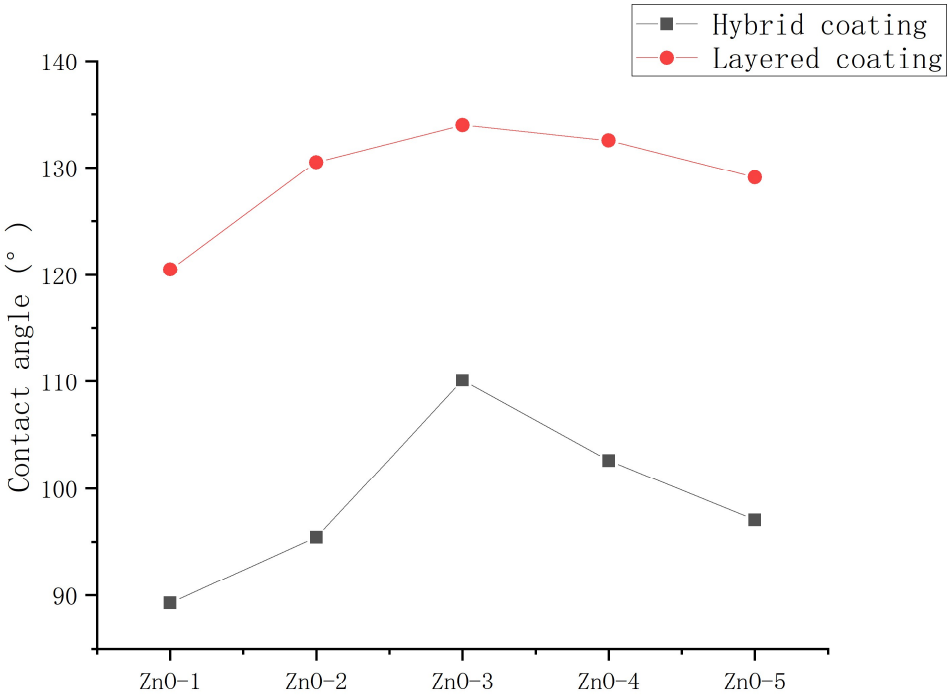

Figure 8. Contact angles of ZnO/epoxy hybrid coating and ZnO/epoxy layered coating.

To sum up, the preparation method of nanoparticle/epoxy coating was: ultrasonic dispersion and layered spraying.

3.2. Contact angles of asphalt concrete with nanocomposite coatings

3.2.1. Influence of mass ratio of nanoparticles to stearic acid on contact angle

Figure 9 shows the contact angles of coatings with different mass ratios of nanoparticles to stearic acid. The mass ratios of stearic acid had a great influence on the contact angles of coatings. Whether ZnO, TiO_2 or SiO_2 nanoparticles, the contact angle increased first and then decreased with the increase of stearic acid. The optimum mass ratios of nanoparticles to stearic acid of ZnO, TiO_2 and SiO_2 coatings were 5:0.5, 5:0.75 and 5:0.8, respectively. This may be because if the amount of stearic acid was less than the optimum value, the nanoparticles cannot react with stearic acid sufficiently. On the other hand, if the amount of stearic acid was more than the optimum value, the hydrophilic group carboxyl group in the unreacted stearic acid reduced the hydrophilicity of the coating [24].

Preprints (www.preprints.org) | NOT PEER-REVIEWED | Posted: 15 September 2023 doi:10.20944/preprints202309.0981.v1

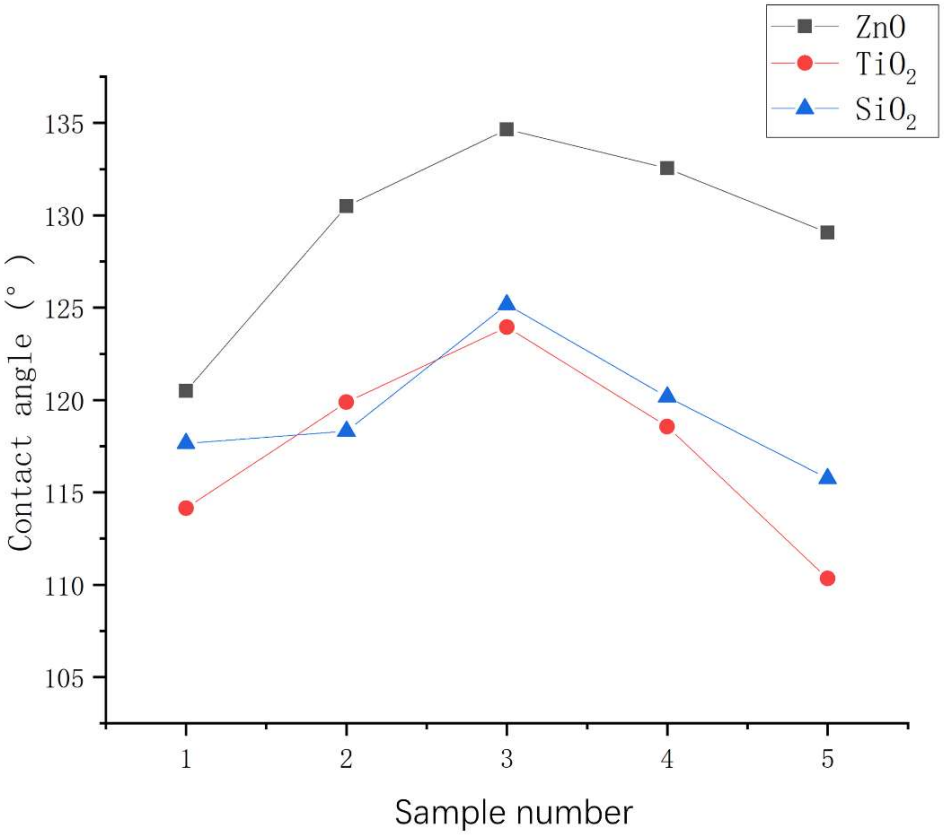

Figure 9. Contact angles of coatings with different mass ratios of nanoparticles to stearic acid.

3.2.2. Influence of dosage of nanoparticle to hydrophobic materials on contact angle

Figure 10 shows the contact angles of asphalt concrete with different dosages of nano-ZnO, nano-TiO_2 and nano-SiO_2. The contact angle increased first and then decreased with the increase of nanoparticle dosage. It is possible that, as the nanoparticle content increases, the aggregation of nanoparticles becomes more serious, which makes the dispersion of nanoparticles more difficult and the hydrophobicity growth rate of the coating worse[16]. Moreover, in corresponding dosages of nanoparticle of 2.0, 3.0, and 4.0 wt% for ZnO, TiO_2 and SiO_2 coating, contact angles of three types of coated concrete reached their maximum values of 137.6°, 119.6°, and 121.0°, respectively.

Preprints (www.preprints.org) | NOT PEER-REVIEWED | Posted: 15 September 2023 doi:10.20944/preprints202309.0981.v1

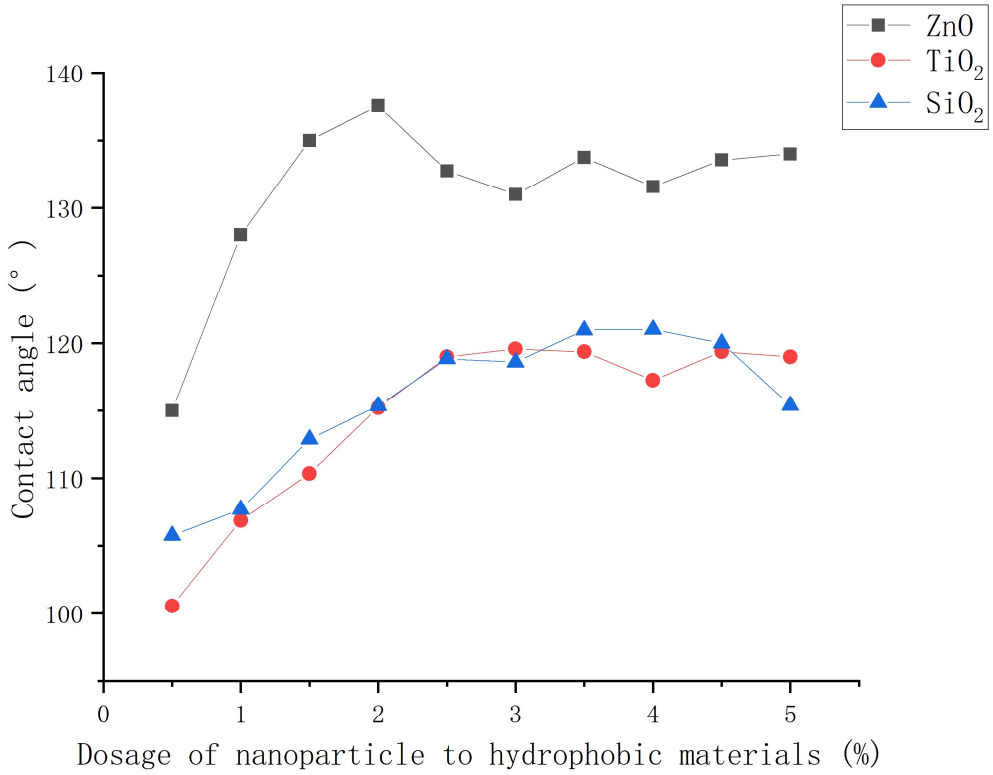

Figure 10. Contact angles of coatings with different dosages of nanoparticle to hydrophobic materials.

Given the amount that exceeded the optimal amount, contact angles of nano-ZnO coating decreased greatly, whereas those of nano-TiO_2 and nano-SiO_2 were stabilized. In comparison with nano-TiO_2 and nano-SiO_2, nano-ZnO was more effective in improving contact angles and saving nanoparticles.

3.3. Fourier transform infrared (FT-IR) spectroscopy analysis

To investigate the effect of different nanomaterials on the hydrophobicity of the coating, the molecular structure of the coatings was analyzed using FTIR.

As shown in Figure 11, the peaks at 2919 and 2850 cm^{-1} were assigned to the asymmetric stretching vibration absorption of C–H of the alkyl group in stearic acid, indicating that the alkyl group in stearic acid was grafted onto the nanoparticle surface [27]. The peaks at 2919 and 2850 cm^{-1} were assigned to the bending vibration of O–H, which indicates that there were hydroxyl groups and adsorbed water on the surface of SiO_2 [31]. The peak at 1707 cm^{-1} was assigned to the stretching vibration absorption of C=O. Since the absorption peak of the C=O functional group is a typical absorption peak in the molecular structure of stearic acid [28], the existence of C=O functional group in the nanoparticle FTIR spectra indicates that stearic acid was successfully connected to the surface of the nanoparticles.

Preprints (www.preprints.org) | NOT PEER-REVIEWED | Posted: 15 September 2023 doi:10.20944/preprints202309.0981.v1

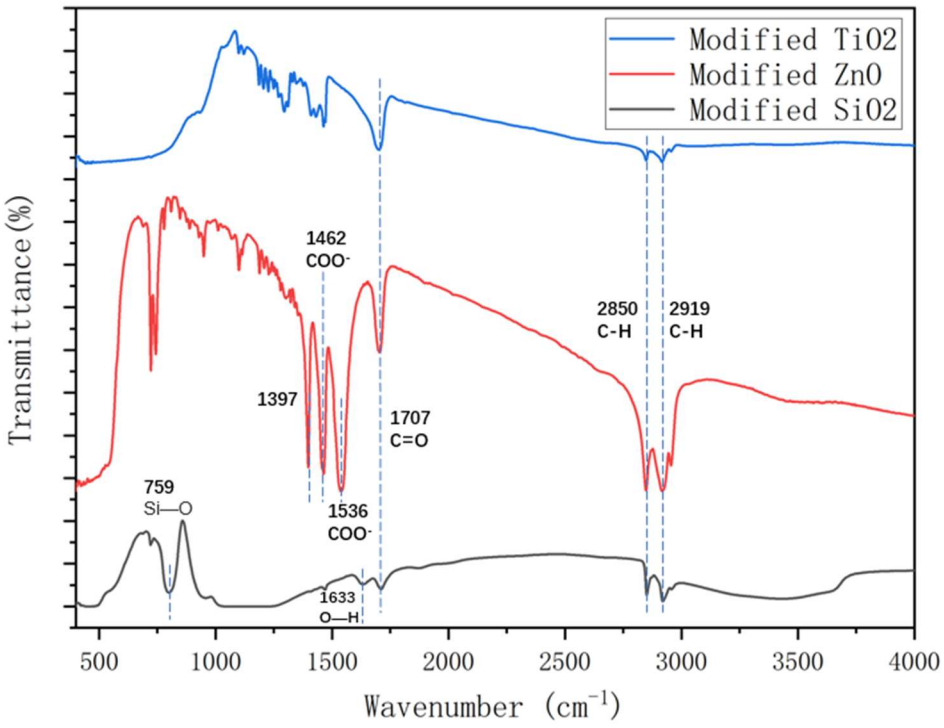

Figure 11. FTIR spectra for modified TiO_2, ZnO, and SiO_2.

It was found that the peak areas of TiO_2 and SiO_2 were significantly smaller than that of ZnO, indicating that the reaction degree of TiO_2 and SiO_2 with stearic acid was significantly lower than that of ZnO. This could explain the poorer hydrophobicity of TiO_2 and SiO_2 coatings.

3.4. Scanning electron microscopy (SEM) analysis

Surface roughness is an important factor affecting the hydrophobicity of the coating. According to the Cassie model [32], the solid rough surface is a composite surface with a three-phase composite contact of "solid–liquid–gas." In particular, part of the air resides between the solid rough surface and the water droplet, which increases the contact angle and achieves hydrophobic properties. As shown in Figure 12, there are serious differences in the roughness of the surface of each coating. The surface of TiO_2/epoxy hybrid coating and epoxy coating is smooth. There are some small potholes, but the surface roughness is not enough. The surface of ZnO, SiO_2 and TiO_2 coating is covered with nanoparticles, which are interlaced with each other, and there are enough voids to create conditions for an increase in the contact angle. The ZnO/epoxy layered coating has a layered structure. According to the SEM image, the white bumps are modified zinc oxide particles and the black smooth part is epoxy resin. The uneven zinc oxide particles improve the hydrophobicity, and the underlying epoxy resin ensures the coating adhesion and abrasion resistance.

Preprints (www.preprints.org) | NOT PEER-REVIEWED | Posted: 15 September 2023 doi:10.20944/preprints202309.0981.v1

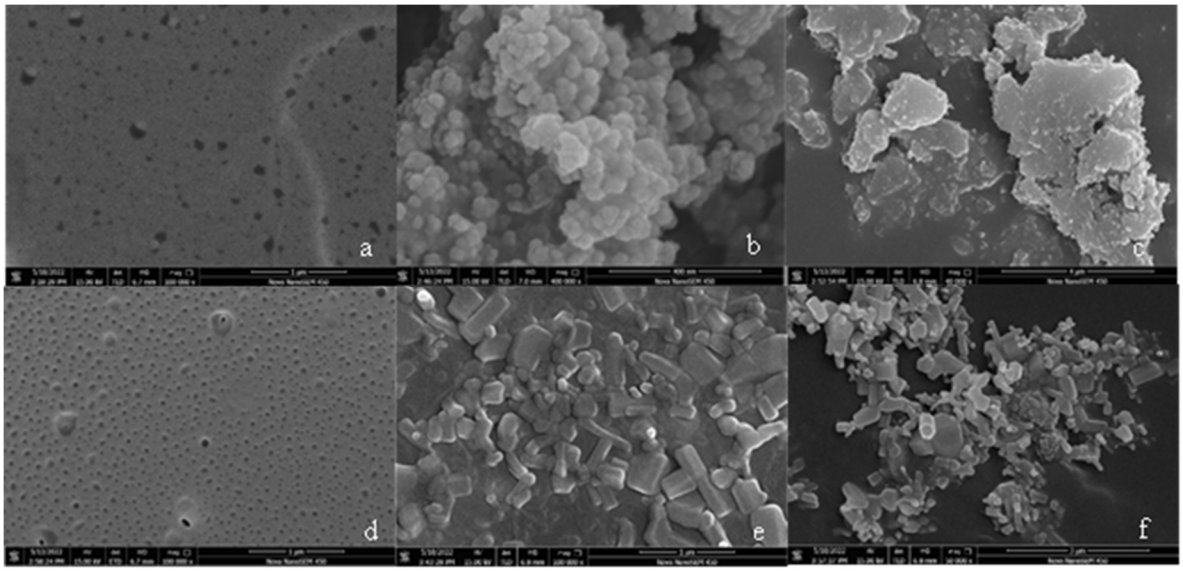

Figure 12. Scanning electron microscopy image (a) TiO_2/epoxy hybrid coating; (b) SiO_2 coating; (c) TiO_2 coating; (d) epoxy coating; (e) ZnO coating; and (f) ZnO/epoxy layered coating.

3.5. Ice adhesion force of asphalt concrete with nanocomposite coatings

The adhesion strength was characterized using Eq (1)

$$\tau_{ice} = F/A \quad (1)$$

where τ_{ice} is adhesion strength, (KPa); F represents the adhesion force, (kN); A depicts the area of ice (m^2), $A=\pi R^2=3.14* 0.10162/2m^2=0.00811\ m^2$.

The adhesion strength between ice and coating under different nanoparticle dosages was tested. The results are shown in Figure 13.

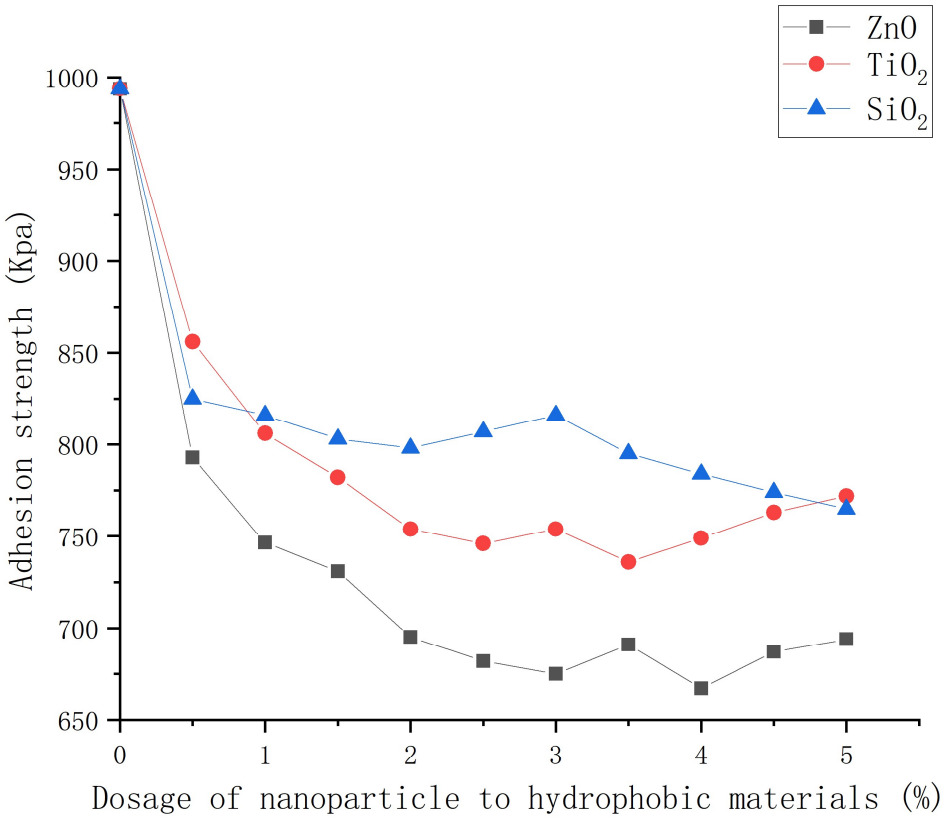

Preprints (www.preprints.org) | NOT PEER-REVIEWED | Posted: 15 September 2023 doi:10.20944/preprints202309.0981.v1

Figure 13. Adhesion strength of coatings with different dosages of nanoparticle to hydrophobic materials.

From Figure 13, it can be seen that, overall, for asphalt concrete with three hydrophobic coatings, the adhesion strength of ice and pavement decreased with the increase of nanoparticle dosage. However, when the dosage of ZnO nanoparticle was higher than 4% or the dosage of TiO_2 nanoparticle was higher than 3.5%, the adhesion strength showed an upward trend, so, a dosage of nanoparticle is not necessary. Moreover, when the dosages of nanoparticle were 4.0, 3.5, and 5.0 wt% for ZnO, TiO_2 and SiO_2 coating reaches 20%, the adhesion strength of three types of coated concrete reached their minimum values of 667, 736 and 764Kpa, respectively. ZnO, TiO_2 and SiO_2 coatings helped reduce the adhesion strength by 32.4%, 25.4%, and 22.6% compared with that of ordinary asphalt concrete. Overall, ZnO hydrophobic coating has the best effect of reducing adhesion and moderate dosage.

3.6. Icing rate of asphalt concrete with nanoparticle coatings

The icing rates of water on the asphalt concrete with the optimum dosages of nanoparticle to hydrophobic materials (2.0, 3.0, and 4.0 wt% for ZnO, TiO_2 and SiO_2 coating) were measured at −10, −6, and −2 °C. The test results are shown in Figure 14.

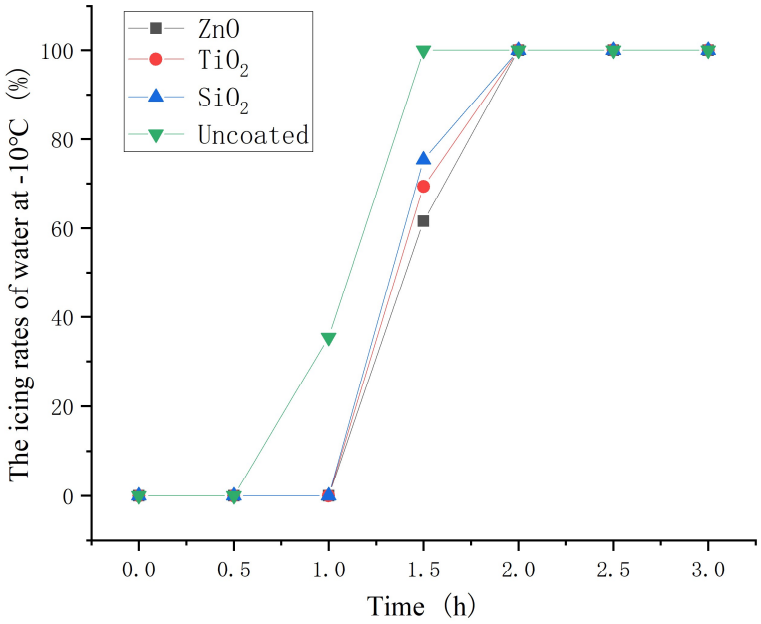

(a)

Preprints (www.preprints.org) | NOT PEER-REVIEWED | Posted: 15 September 2023 doi:10.20944/preprints202309.0981.v1

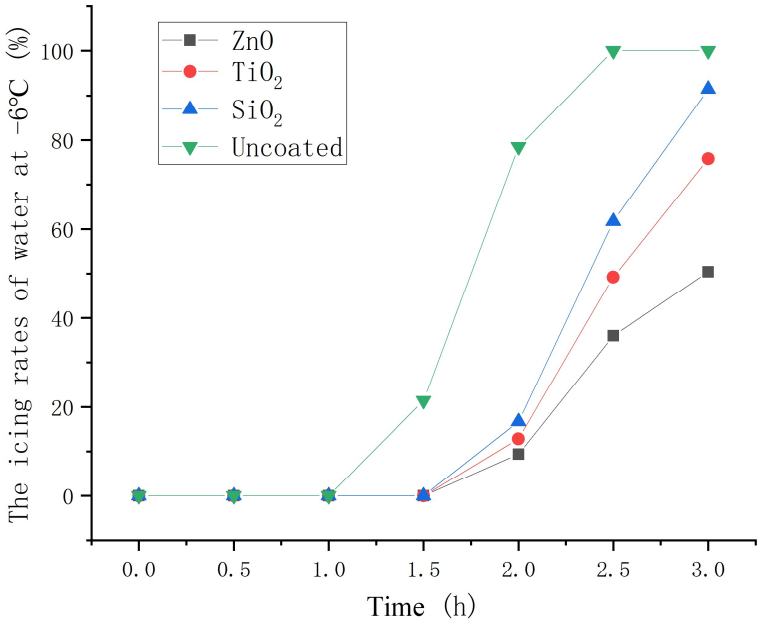

(b)

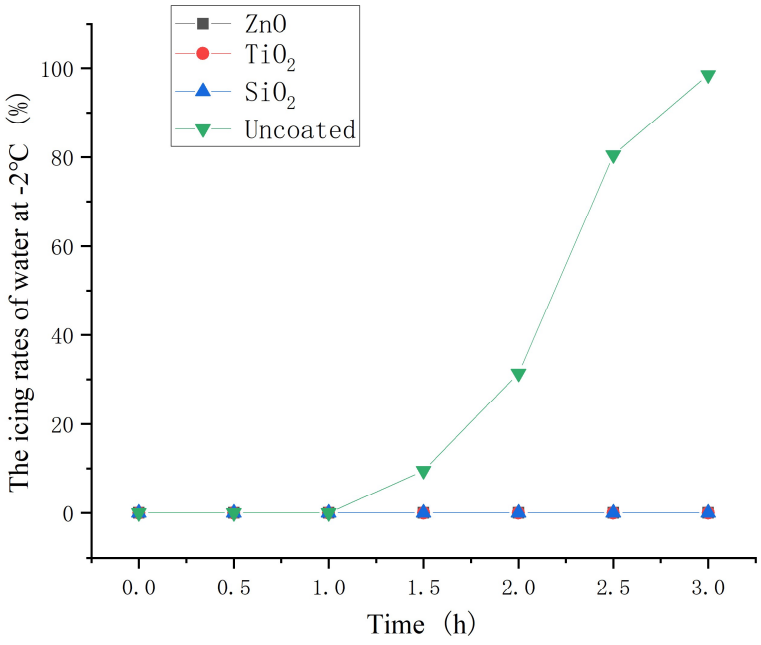

(c)

Figure 14. Icing rates of water on different asphalt concrete at (a) −10°C; (b) −6°C; and (c) −2°C.

As shown in Figure 14, The beginning icing time of coated asphalt concrete was significantly later than that of uncoated asphalt concrete, and the icing rate of coated asphalt concrete was less than that of uncoated asphalt concrete at the same point in time. This indicates that the hydrophobic coating has a good inhibiting effect on icing. Moreover, the inhibiting effect on icing of ZnO, TiO_2

Preprints (www.preprints.org) | NOT PEER-REVIEWED | Posted: 15 September 2023 doi:10.20944/preprints202309.0981.v1

and SiO_2 hydrophobic coating decrease in turn. In the environment of −10 and −2°C, hydrophobic coating delayed the beginning icing time by up to 30min and at least 2 hours, respectively. Therefore, the hydrophobic coating can help delay icing, thereby reducing the amount of ice on the road and buying time for deicing.

3.7. Contact angle attenuation of coatings with different epoxy resin contents

The test results of contact angles of coatings with different mass ratios of epoxy resin to nanoparticle over time are shown in Figure 15. It can be seen that the contact angle of the coating was gradually reduced due to the effect of vehicle load and environment, which indicates that the hydrophobicity of the coating was reduced. Moreover, the contact angle decreased with the increased dosage of the mass ratio of epoxy resin to nanoparticle, indicating that the epoxy resin significantly improved the durability of the coating. However, coatings with higher dosages of epoxy resin had smaller contact angles. Possibly, with increasing dosage of epoxy resin, epoxy resin fills the gap between nanoparticles and water droplets, reducing the hydrophobicity of the coating.

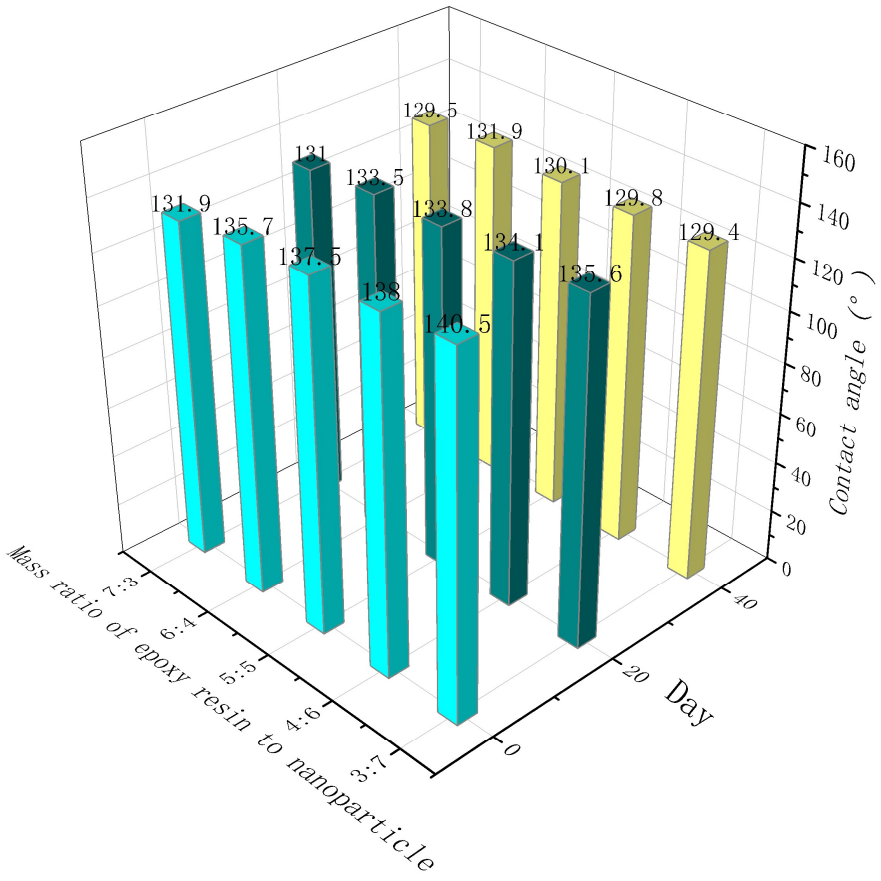

Figure 15. Contact angles of coatings with different mass ratios of epoxy resin to nanoparticle over time.

3.8. Mechanism of modified nanoparticles and epoxy resin

Figure 16 shows the improvement mechanism of modified nanoparticles and epoxy resin on hydrophobicity and durability of coating. Modification of stearic acid makes nanoparticles hydrophobic. According to Cassie's theory [33], the water droplets cannot fill the air cavity between the droplets and the pavement. The existence of the air cavity on the contact surface prevents the ice layer from being in close contact with the road surface, which reduces the contact area and adhesive force, and improves road anti-icing performance[34].

Preprints (www.preprints.org) | NOT PEER-REVIEWED | Posted: 15 September 2023 doi:10.20944/preprints202309.0981.v1

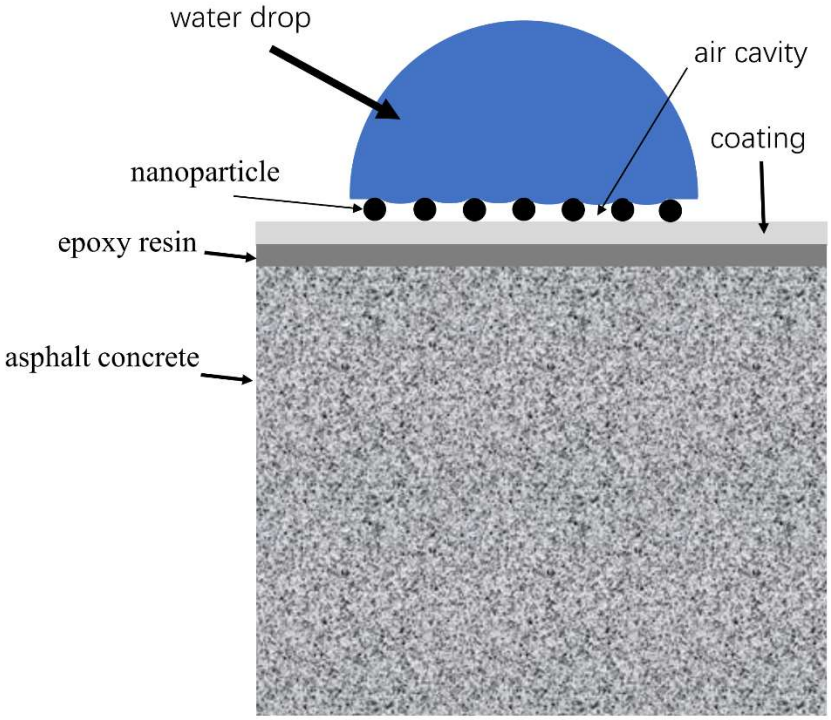

Figure 16. The improvement mechanism of modified nanoparticles and epoxy resin on hydrophobicity and durability of coating.

The hydrophobic ice coating has low adhesion strength with the pavement and is easy to wear. The epoxy resin layer is used as the bonding layer between the pavement and coating to avoid peeling under the combined action of vehicle load and environment. However, Too much epoxy resin will cover the cavity in the nanoparticles, reducing the hydrophobicity of the coating.

4. Conclusions

Based on the results and analysis, the following main conclusions can be drawn.

1. Nano-ZnO, TiO_2 and SiO_2 particles can be modified into hydrophobicity by stearic acid. The optimum preparation method of nanoparticle/epoxy coating is: ultrasonic dispersion and layered spraying.
2. The mass ratio of nanoparticles to stearic acid and dosage of nanoparticle to hydrophobic materials have a significant impact on the contact angle of hydrophobic coating. The contact angle increases first and then decreases with the increase of stearic acid. The contact angle increases first and then decreases with the increase of nanoparticle dosage.
3. The FTIR test shows that during the chemical reactions of zinc oxide with stearic acid, the carboxyl group in stearic acid was esterified with the hydroxyl group in zinc oxide, which made ZnO nanoparticles disperse more efficiently. In addition, ultrasonic dispersion could increase the reaction degree significantly. The reaction degree of TiO_2 and SiO_2 with stearic acid was lower than that of ZnO, which could explain the poor hydrophobicity of TiO_2 and SiO_2 coatings.
4. The SEM test shows that the surface of coating is covered with nanoparticles, which are interlaced with each other to form a rough hydrophobic surface. In addition, the ZnO/epoxy layered coating have a layered structure. The lower layer of epoxy resin solution can enhance the durability of the coating, and the upper layer of zinc oxide solution can form a rough hydrophobic surface.

5. The hydrophobic coating can reduce the adhesion strength of ice and asphalt concrete, which decreases with the increase of nanoparticle dosage. ZnO, TiO_2 and SiO_2 coatings can help reduce the adhesion strength by 32.4%, 25.4%, and 22.6% compared with that of ordinary asphalt concrete.
6. The hydrophobic coating has a good inhibiting effect on icing. Moreover, the inhibiting effect on icing of ZnO, TiO_2 and SiO_2 hydrophobic coating decrease in turn. In the environment of −10 and −2°C, hydrophobic coating delayed the beginning icing time by up to 30min and at least 2 hours, respectively.
7. The contact angle decreased with the increased dosage of the mass ratio of epoxy resin to nanoparticle, indicating that the epoxy resin significantly improved the durability of the coating. However, coatings with higher dosages of epoxy resin had smaller contact angles. Possibly, with increasing dosage of epoxy resin, epoxy resin fills the gap between nanoparticles and water droplets, reducing the hydrophobicity of the coating.

Acknowledgments: This research was financially supported by National Key R&D Program of China (Grant No. 2021YFB2601200), National Natural Science Foundation of China (No. 52308445, No. 51778140, No. 52078130), Major Technology Demonstration of Epoxy Asphalt in Pavement as a Green Highly Efficient Carbon Mitigation Technology of Jiangsu, China (Major Technology Demonstration Program) (No. BE2022615), Major Science and Technology Project of Nanjing (No. 202209012), Technology Research and Development Program of China State Railway Group Co., Ltd.(Beijing 10000, China) (P2019G030).

References

1. Boinovich, L.B.; Emelyanenko, A.M. Anti-icing Potential of Superhydrophobic Coatings. *Mendeleev Communications* **2013**, *23*, 3-10, doi:https://doi.org/10.1016/j.mencom.2013.01.002.
2. Laforte, J.L.; Allaire, M.A.; Laflamme, J. Wind tunnel evaluation of a rime metering device using a magnetostrictive sensor. *Atmospheric Research* **1995**, *36*, 287-301, doi:https://doi.org/10.1016/0169-8095(94)00043-D.
3. Li, J.; Luo, Y.; Zhu, J.; Li, H.; Gao, X. Subcooled-Water Nonstickiness of Condensate Microdrop Self-Propelling Nanosurfaces. *ACS Applied Materials & Interfaces* **2015**, *7*, 26391-26395, doi:10.1021/acsami.5b09719.
4. Li, Q.; Guo, Z.G. Fundamentals of icing and common strategies for designing biomimetic anti-icing surfaces. *Journal of Materials Chemistry A* **2018**, *6*, 13549-13581, doi:10.1039/c8ta03259a.
5. Guo, P.; Zheng, Y.M.; Wen, M.X.; Song, C.; Lin, Y.C.; Jiang, L. Icephobic/Anti-Icing Properties of Micro/Nanostructured Surfaces. *Advanced Materials* **2012**, *24*, 2642-2648, doi:10.1002/adma.201104412.
6. Wu, X.H.; Chen, Z. A mechanically robust transparent coating for anti-icing and self-cleaning applications. *Journal of Materials Chemistry A* **2018**, *6*, 16043-16052, doi:10.1039/c8ta05692g.
7. Zhang, S.N.; Huang, J.Y.; Chen, Z.; Yang, S.; Lai, Y.K. Liquid mobility on superwettable surfaces for applications in energy and the environment. *Journal of Materials Chemistry A* **2019**, *7*, 38-63, doi:10.1039/c8ta09403a.
8. Wu, X.H.; Zhao, X.; Ho, J.W.C.; Chen, Z. Design and durability study of environmental-friendly room-temperature processable icephobic coatings. *Chemical Engineering Journal* **2019**, *355*, 901-909, doi:10.1016/j.cej.2018.07.204.
9. Barthlott, W.; Neinhuis, C. Purity of the sacred lotus, or escape from contamination in biological surfaces. *Planta* **1997**, *202*, 1-8, doi:10.1007/s004250050096.
10. Laforte, C.; Laforte, J.; Carrière, J. How a solid coating can reduce the adhesion of ice on a structure. In Proceedings of the Proceedings of the international workshop on atmospheric icing of structures (IWAIS), 2002.
11. Arabzadeh, A.; Ceylan, H.; Kim, S.; Gopalakrishnan, K.; Sassani, A. Superhydrophobic Coatings on Asphalt Concrete Surfaces: Toward Smart Solutions for Winter Pavement Maintenance. *Transportation Research Record* **2016**, *2551*, 10-17, doi:10.3141/2551-02.
12. Ruan, M.; Li, W.; Wang, B.; Deng, B.; Ma, F.; Yu, Z. Preparation and anti-icing behavior of superhydrophobic surfaces on aluminum alloy substrates. *Langmuir* **2013**, *29*, 8482-8491.
13. Yang, J.; Li, W. Preparation of superhydrophobic surfaces on Al substrates and the anti-icing behavior. *Journal of Alloys and Compounds* **2013**, *576*, 215-219.
14. Antonini, C.; Innocenti, M.; Horn, T.; Marengo, M.; Amirfazli, A. Understanding the effect of superhydrophobic coatings on energy reduction in anti-icing systems. *Cold regions science and technology* **2011**, *67*, 58-67.

15. Dotan, A.; Dodiuk, H.; Laforte, C.; Kenig, S. The relationship between water wetting and ice adhesion. *Journal of Adhesion Science and Technology* **2009**, *23*, 1907-1915.
16. Li, G.; Yue, J.; Guo, C.; Ji, Y. Influences of modified nanoparticles on hydrophobicity of concrete with organic film coating. *Construction and Building Materials* **2018**, *169*, 1-7, doi:https://doi.org/10.1016/j.conbuildmat.2018.02.191.
17. Peng, C.; Hu, Y.; You, Z.; Yang, H.; Nie, Y.; Wu, T.; Yang, H.; Ou, R. Preparation and anti-icing performance of acrylic superhydrophobic asphalt pavement coating with microwave heating function. *Construction and Building Materials* **2022**, *344*, 128289, doi:https://doi.org/10.1016/j.conbuildmat.2022.128289.
18. Zhang, D.; Wang, L.; Qian, H.; Li, X. Superhydrophobic surfaces for corrosion protection: a review of recent progresses and future directions. *Journal of Coatings Technology and Research* **2016**, *13*, 11-29, doi:10.1007/s11998-015-9744-6.
19. Li, X.; Cao, Z.; Zhang, Z.; Dang, H. Surface-modification in situ of nano-SiO2 and its structure and tribological properties. *Applied Surface Science* **2006**, *252*, 7856-7861, doi:https://doi.org/10.1016/j.apsusc.2005.09.068.
20. Schmidt, D.F.; Giannelis, E.P. Silicate Dispersion and Mechanical Reinforcement in Polysiloxane/Layered Silicate Nanocomposites. *Chemistry of Materials* **2010**, *22*, 167-174, doi:10.1021/cm9026978.
21. He, F.Q.; Zhao, Y.P. Growth of ZnO nanotetrapods with hexagonal crown. *Applied Physics Letters* **2006**, *88*, doi:10.1063/1.2202003.
22. Wang, B.-B.; Feng, J.-T.; Zhao, Y.-P.; Yu, T.X. Fabrication of Novel Superhydrophobic Surfaces and Water Droplet Bouncing Behavior — Part 1: Stable ZnO–PDMS Superhydrophobic Surface with Low Hysteresis Constructed Using ZnO Nanoparticles. *Journal of Adhesion Science and Technology* **2010**, *24*, 2693-2705, doi:10.1163/016942410X508244.
23. Wang, B.B.; Zhao, Y.P.; Yu, T.X. Fabrication of Novel Superhydrophobic Surfaces and Droplet Bouncing Behavior - Part 2: Water Droplet Impact Experiment on Superhydrophobic Surfaces Constructed Using ZnO Nanoparticles. *Journal of Adhesion Science and Technology* **2011**, *25*, 93-108, doi:10.1163/016942410x501115.
24. Ding, B.; Ogawa, T.; Kim, J.; Fujimoto, K.; Shiratori, S. Fabrication of a super-hydrophobic nanofibrous zinc oxide film surface by electrospinning. *Thin Solid Films* **2008**, *516*, 2495-2501, doi:10.1016/j.tsf.2007.04.086.
25. Wu, X.; Chen, Z. A mechanically robust transparent coating for anti-icing and self-cleaning applications. *Journal of Materials Chemistry A* **2018**, *6*, 16043-16052, doi:10.1039/C8TA05692G.
26. Zhuo, Y.; Håkonsen, V.; He, Z.; Xiao, S.; He, J.; Zhang, Z. Enhancing the Mechanical Durability of Icephobic Surfaces by Introducing Autonomous Self-Healing Function. *ACS Applied Materials & Interfaces* **2018**, *10*, 11972-11978, doi:10.1021/acsami.8b01866.
27. Gao, W.; Zhou, B.; Liu, Y.H.; Ma, X.Y.; Liu, Y.; Wang, Z.C.; Zhu, Y.C. The influence of surface modification on the structure and properties of a zinc oxide-filled poly(ethylene terephthalate). *Polymer International* **2013**, *62*, 432-438, doi:10.1002/pi.4328.
28. Zhu, W.K.; Wu, Y.; Zhang, Y. Fabrication and characterization of superhydrophobicity ZnO nanoparticles with two morphologies by using stearic acid. *Materials Research Express* **2019**, *6*, doi:10.1088/2053-1591/ab4ec5.
29. Ma, F.; Chen, S.; Liu, P.; Geng, F.; Li, W.; Liu, X.; He, D.; Pan, D. Improvement of β-TCP/PLLA biodegradable material by surface modification with stearic acid. *Materials Science and Engineering: C* **2016**, *62*, 407-413, doi:https://doi.org/10.1016/j.msec.2016.01.087.
30. Arfaoui, M.A.; Dolez, P.I.; Dube, M.; David, E. Development and characterization of a hydrophobic treatment for jute fibres based on zinc oxide nanoparticles and a fatty acid. *Applied Surface Science* **2017**, *397*, 19-29, doi:10.1016/j.apsusc.2016.11.085.
31. Zheng, C.; Cheng, Y.M.; Wei, Q.B.; Li, X.H.; Zhang, Z.J. Suspension of surface-modified nano-SiO2 in partially hydrolyzed aqueous solution of polyacrylamide for enhanced oil recovery. *Colloids and Surfaces a-Physicochemical and Engineering Aspects* **2017**, *524*, 169-177, doi:10.1016/j.colsurfa.2017.04.026.
32. Choi, W.; Tuteja, A.; Mabry, J.M.; Cohen, R.E.; McKinley, G.H. A modified Cassie–Baxter relationship to explain contact angle hysteresis and anisotropy on non-wetting textured surfaces. *Journal of colloid and interface science* **2009**, *339*, 208-216.
33. Cassie, A.; Baxter, S. Wettability of porous surfaces. *Transactions of the Faraday society* **1944**, *40*, 546-551.
34. Kreder, M.J.; Alvarenga, J.; Kim, P.; Aizenberg, J. Design of anti-icing surfaces: smooth, textured or slippery? *Nature Reviews Materials* **2016**, *1*, 15003, doi:10.1038/natrevmats.2015.3.